Marine Environmental Research 78 (2012) 15–25

Contents lists available at SciVerse ScienceDirect

Marine Environmental Research

journal homepage: www.elsevier.com/locate/marenvrev

Specific pathways for the incorporation of dissolved barium and molybdenum into the bivalve shell: An isotopic tracer approach in the juvenile Great Scallop (*Pecten maximus*)

Hélène Tabouret [a,*], Sébastien Pomerleau [a,c], Aurélie Jolivet [b], Christophe Pécheyran [a], Ricardo Riso [b], Julien Thébault [b], Laurent Chauvaud [b], David Amouroux [a]

[a] *Laboratoire de Chimie Analytique Bio-Inorganique et Environnement, Institut des Sciences Analytiques et de Physico-Chimie pour l'Environnement et les Matériaux, UMR 5254 CNRS – Université de Pau et des Pays de l'Adour, Pau, France*
[b] *Université de Brest, Laboratoire des Sciences de l'Environnement Marin (UMR CNRS/IRD/UBO 6539), Institut Européen de la Mer, technopôle Brest-Iroise, Plouzané, France*
[c] *Université du Québec, Département de Chimie, Biologie et Géographie, Rimouski, Québec, Canada G5L3A1*

ARTICLE INFO

Article history:
Received 1 December 2011
Received in revised form
22 March 2012
Accepted 23 March 2012

Keywords:
Isotopes
Femtosecond laser ablation
Scallop shell
Barium
Molybdenum
Pecten maximus
Tracers
Biogeochemical cycle

ABSTRACT

Dissolved barium and molybdenum incorporation in the calcite shell was investigated in the Great Scallop *Pecten maximus*. Sixty six individuals were exposed for 16 days to two successive dissolved Ba and Mo concentrations accurately differentiated by two different isotopic enrichments (^{97}Mo, ^{95}Mo; ^{135}Ba, ^{137}Ba). Soft tissue and shell isotopic composition were determined respectively by quantitative ICP-MS (Inductively Coupled Plasma Mass Spectrometer) and laser ablation – ICP-MS. Results from Ba enrichment indicate the direct incorporation of dissolved Ba into the shell in proportion to the levels in the water in which they grew with a 6–8 day delay. The low spike contributions and the low partition coefficient ($D_{Mo} = 0.0049 \pm 0.0013$), show that neither the soft tissue nor the shell were significantly sensitive to Mo enrichment. These results eliminate direct Mo shell enrichment by the dissolved phase, and favour a trophic uptake that will be investigated using the successive isotopic enrichment approach developed in this study.

1. Introduction

For several decades most of the studies dealing with the reconstruction of past variations in ocean productivity have focused on the research of archived proxies in marine sediments: accumulation of calcium carbonate, opal, organic matter, foraminifera assemblage, barite ($BaSO_4$) accumulation rate, barium/titanium (Ba/Ti) and aluminium/titanium (Al/Ti) ratios (Averyt and Paytan, 2004). However the temporal resolution of such reconstructions is too low to take into account all the spatio-temporal variability of the chemical, physical and biological processes occurring on the continental shelf, which contributes to one quarter of the global primary production (Smith and Hollibaugh, 1993). Since the 1960s, researches have focused on mollusc shells as they grow by periodic accretion of calcium carbonate layers. In contrast to coral and varved sediments, most molluscs form distinct and easily discernable circadian, circalunidian, or ultradian growth structures and provide information on sub-seasonal variations of paleo-environmental conditions (Schöne et al., 2005). In the case of the Great Scallop *Pecten maximus*, both seasonal and daily growth bands are produced, providing a record of high temporal resolution, and representing an extraordinary archive due to its wide geographical distribution (Chauvaud et al., 1998, 2005).

Investigations also focused on the potential presence of trace elements in the carbonate matrix as a bio-indicator of environmental conditions experienced by the organism during its life time (Dodd, 1965; Lorens and Bender, 1980; Klein et al., 1996a,b; Stecher et al., 1996; Vander Putten et al., 2000; Gillikin et al., 2006; Barats et al., 2008). Among the elemental signals (e.g., Sr, Mn, Pb, U), many elements cannot be used as proxies of environmental conditions due to strong biological effects (Stecher et al., 1996; Lorrain et al., 2005; Vander Putten et al., 2000; Gillikin et al., 2005; Freitas et al., 2006). However an increasing number of studies investigated the Ba

* Corresponding author. Muséum National d'Histoire Naturelle, Département Milieux et Peuplements aquatiques, Biologie des Organismes marins et Ecosystèmes aquatiques (BOREA UMR CNRS-MNHN 7208), CP-026, 43 rue Cuvier, 75231 Paris, France. Tel.: +33 (0) 1 40 79 80 35; fax: +33 (0) 1 40 79 37 71.
E-mail address: tabouret@mnhn.fr (H. Tabouret).

0141-1136/$ – see front matter © 2012 Elsevier Ltd. All rights reserved.
doi:10.1016/j.marenvres.2012.03.006

signals in shells of *Mytilus edulis* (Vander Putten et al., 2000; Gillikin et al., 2006), *Isognomon ephippium* (Lazareth et al., 2003), *Chione subrugosa* (Carré et al., 2006), clams (*Mercenaria mercenaria*, *Spisula solidissima*, *Artica islandica*, *Mesodesma donacium*, *Saxidomus giganteus*, *Corbicula fluminea*) (Fritz et al., 1990; Stecher et al., 1996; Epplé, 2004; Carré et al., 2006; Gillikin et al., 2008), and scallops (*P. maximus*, *Comptopallium radula*, *Argopecten purpuratus*) (Lorrain, 2002; Gillikin et al., 2008; Barats et al., 2009; Richard, 2009; Thébault et al., 2009). In all these studies the Ba:Ca signal shows a relatively stable background interrupted by sharp episodic peaks. The reproducibility of these sharp peaks between different shells growing at the same location indicates an environmental influence (Vander Putten et al., 2000; Carré et al., 2006; Gillikin et al., 2008; Barats et al., 2009; Thébault et al., 2009). Field and laboratory experiments on *M. edulis* showed that background Ba:Ca ratio in shell was directly caused by Ba:Ca levels in water (Gillikin et al., 2006). The partition coefficient D_{Ba} estimated from field studies on three *P. maximus* supports the link between these two compartments (Barats et al., 2009) but has not yet been confirmed in controlled laboratory experiments. Ba:Ca maxima in scallop shells was found to occur in summer post-bloom conditions. The explanation of the Ba peaks is confusing. Stecher et al. (1996) proposed that Ba maxima in shells might be induced by the ingestion of Ba-rich phytoplankton or barite formed in decaying phytoplankton aggregates. Data obtained on *M. edulis* (Gillikin et al., 2006) and *P. maximus* (Barats et al., 2009) did not support the direct incorporation of Ba from phytoplankton ingestion into the shell and indicates that Ba:Ca ratio in shell cannot be used as a proxy of phytoplankton production. Another explanation given by authors, are short increases in dissolved Ba, biological partitioning of Ba to calcification sites, or differences in shell microstructure (Gillikin et al., 2008). These peaks are not considered to correlate to riverine discharge in contrast to coral (McCulloch et al., 2003; Sinclair and McCulloch, 2004) and are thought to be caused by a "biogenic" influence (Gillikin et al., 2008; Barats et al., 2009) subsequent to specific phytoplankton blooms.

Recently, the analyses of scallop shells revealed the potential of another element: molybdenum (Mo) (Richard, 2009; Thébault et al., 2009; Barats et al., 2010). The seasonal Mo pattern in shell was similar to the pattern described for Ba with low constant background, interrupted by transient enrichments occurring from May to June in *P. maximus* (Barats et al., 2010). This pattern was reproducible in individuals from the same population (Barats et al., 2010). Mo maxima in *P. maximus* were observed after a significant increase in dissolved Mo, which was found to be directly influenced by changes in environmental conditions at the sediment water interface (SWI) occurring after the intense and periodic spring bloom (Barats et al., 2010). Thébault et al. (2009) suggested that the maxima could be the result of the ingestion of phytoplankton cells grown on nitrates and containing high levels of Mo required to support the activity of nitrate reductase. In addition, Barats et al. (2010) have shown that Mo shell enrichment in the Bay of Brest (France) was directly correlated to silicate and nitrate removal in spring, after major seasonal diatom blooms, confirming a strong and specific pelagic biological control. Until now, no experiment has been designed to better understand the Mo accumulation pathway in shell and to better define the contribution of the dissolved and particulate fractions.

The aim of this study was to assess if the calcite shell of Great Scallop, *P. maximus*, incorporates Ba and Mo in proportion to the levels in the water in which they grew. Young individuals were exposed to different levels of dissolved Ba and Mo in the laboratory. The concentration increase was produced by two successive enrichments (spikes) of different Mo (^{97}Mo; ^{95}Mo) and Ba (^{135}Ba; ^{137}Ba) isotopes in order to follow the incorporation in both soft tissue and shell. Results were compared to those obtained in previous field studies to better define the incorporation pathways.

2. Materiel and methods

2.1. Preparation of the isotopically enriched solutions

The first Mo spike solution was prepared with 3.9 mg of ^{97}Mo powder (Eurisotop, St-Aubin, France; purity: 96.6%). The powder was dissolved in 1 ml HNO_3 Normapur 65% (Prolabo) at 100 °C for 1 h. Then, 1 ml H_2O_2 Suprapur, (Prolabo) was added at ambient temperature. The solution was made up to 10 ml with pure water (18.2 MΩ MQ water; Millipore). The same protocol was used for the second Mo spike solution with 7.5 mg of ^{95}Mo powder (Eurisotop, St-Aubin, France; purity: 95.4%). Both ^{135}Ba (4.5 mg, first spike) and ^{137}Ba (8.6 mg, second spike) powders (Eurisotop, St-Aubin, France; purity: 95% and 91.8% respectively) were dissolved with 100 µl HNO_3 Normapur 65%, (Prolabo) and made up to 10 ml with pure water 18.2 MΩ. The final concentrations were calculated to give the natural concentrations needed to induce a Ba or Mo peak in the scallop shell according to the partition coefficients D_{Ba} and D_{Mo} published before this study (Thébault et al., 2009; Barats et al., 2009, 2010). The isotopic ratios of the first spikes were ^{135}Ba/^{138}Ba: 47.214 for the Ba spike and ^{97}Mo/^{98}Mo: 124.060 for the Mo spike. The isotopic ratios of the second spikes were ^{137}Ba/^{138}Ba: 14.669 for the Ba spike and ^{95}Mo/^{98}Mo: 146.769 for the Mo spike.

2.2. Laboratory experiment

For the enrichment experiment 66 young Great Scallops (*P. maximus*) (mean length: 30.04 ± 2.70 mm; max = 34.90 mm; min = 22.45 mm) were collected in the Bay of Brest (France) on 30th April 2010 and placed in a 150 L tank containing sand filtered seawater. The water, collected in the Bay of Brest was continuously circulated. As the sampling of the scallops from the natural environment induces growth inhibition, the individuals were acclimatized to laboratory conditions until shell growth resumed. As the Great Scallop is very sensitive to any manipulation, the point at which growth stopped was the only visible indicator and was used to mark the beginning of the experiment. During the acclimatisation the scallops were continuously fed everyday with a phytoplankton mix (Tahitian *Isochrysis*, *Pavlova lutheri*, *Skeletonema costatum*, 300 × 10^6 cells ml^{-1} per species; Ecloserie du Tinduff, France). On 17th May, taken as the first day of the experiment, the scallops were divided into two tanks containing 142 L sand filtered seawater. Aquarium air pumps ensured the water oxygenation. The first tank was dedicated to the Mo enrichment and the second tank to the Ba enrichment. The Mo tank was used as a control for the Ba experiment and the Ba tank as a control for the Mo experiment. In each tank, a YSI multi-parameter probe, recorded oxygen concentration, temperature and salinity of the water every 5 min. On Day 3, ^{97}Mo and ^{135}Ba solutions were added to the Mo and Ba tanks respectively. The second enrichment with ^{95}Mo and ^{137}Ba solutions occurred on Day 9. The experiment was stopped on Day 16; the experiment was originally designed for 15 days. During the experiment, the scallops were fed with 200 ml of the same phytoplankton mix (300 × 10^6 cells ml^{-1} per species) each day. Previously, the Mo and Ba concentrations of a phytoplankton mix aliquot were measured and were considered negligible (Mo ~ 0.3 nmol l^{-1}; Ba ~ 0.2 nmol l^{-1}). The cell concentration of the phytoplankton mix was sufficiently low to be quickly filtered by all the individuals. The scallop feeding during the enrichment period was kept up to ensure the continuous growth of the individuals. Daily feeding occurred three hours after the spikes and the sampling described below.

2.3. Water, soft tissue and shell sampling

In each tank, 200 ml of water were sampled daily using a 50 ml syringe. 100 ml were filtered directly through a 0.2 μm Minisart RC filter (Sartorius, Germany) in order to investigate the isotopic concentrations of the filtered fraction called "dissolved phase" in this work. 100 ml were placed in a vial without any filtration to determine the bulk water concentrations exhibiting both "dissolved" and "particulate" fractions. On Days 3 and 9, the sampling occurred 20 min after the spike in order to complete the homogenization of the water. Both water samples were directly acidified with 1 ml of HNO_3 65% ultrex (J.T. Baker) and kept at 2 °C until analysis. For the first 10 days, 3 scallops were sampled every two days from each tank. Since no mortality was observed during this period, 3 individuals were sampled everyday from the 11th day until the end of the experiment. The gills, mantle, adductor muscle, digestive gland and the remaining tissues or "the rest" (intestine, kidney) were carefully removed from each individual. Each tissue was weighed and freeze dried. The scallop shells were carefully rinsed with MilliQ water and dried. Clean methods were applied throughout the water sampling, dissection, preparation and analysis by using nitric acid-washed instruments, wearing latex gloves and using 18.2 MΩ MQ water at all stages of the processes to minimize possible exogenous contamination.

A condition index was calculated to check the evolution of the scallop health during the experiment:

$$\text{C.I.} = \text{dry soft tissue weight}/(\text{dry soft tissue weight} + \text{inferior valve weight}) \quad (1)$$

The superior valve weight was not taken into account as they were affected by epibionts and thus could bias the total body weight.

On the basis of the periodicity of striae formation in *P. maximus*, daily shell growth rates were calculated for each shell by measuring the growth increment width along the axis of maximal growth, using an image analysis technique previously described (Chauvaud et al., 1998). For each sampling date, the average growth rate of all the shells available in the tank up to the sampling date was calculated.

2.4. Water and soft tissue analyses

All water samples ($N = 64$) were diluted with HNO_3 1% to obtain salt content below 2 g L^{-1} prior to the analysis. Artificial seawater with 1.5 salinity was reconstructed and used for the standard curve. Analyses of 7 isotopes (^{95}Mo, ^{97}Mo, ^{98}Mo, ^{135}Ba, ^{137}Ba, ^{138}Ba, ^{115}In) were performed with a Thermo XSeries 2 inductively coupled plasma mass spectrometer (ICP-MS; Thermo Fisher Scientific) using Indium (In) as an internal standard. Standard additions were made to the first samples and the last samples of each tank in order to check for the matrix effect. Certified reference materials (CRM, CASS-4; NRCC, Canada) were treated as the samples and were run to check for precision and accuracy. The detection limits were all below 1 nmol l^{-1}. For the CASS-4 the reproducibility was between 4 and 10.2% for the Mo isotopes and between 1.5 and 2.5% for the Ba isotopes. The results for this CRM displayed recoveries for the Mo ranging from 82 to 97% ($N = 10$). The CASS-4 is not certified for Ba, however the reproducibility for this element was good and the results obtained by standard addition for 10 replicates (53.23 ± 3.43 nmol l^{-1}) were in agreement with those obtained in previous studies (Tabouret et al., 2010; Bareille G., CNRS, Pau-France, *pers. com.*).

Soft tissue was ground in an agate mortar. As the individual tissue samples were very small, the same tissue from the three individuals sampled the same day were mixed together and split in two aliquots of 50–100 mg. Aliquots were digested using 1 ml of HNO_3 Instra 70% (J.T. Baker) at ambient temperature overnight. 1 ml HNO_3 Instra 70% and 1 ml H_2O_2 Ultrex (J.T. Baker) were added and the aliquots were placed at 50 °C for 1 h and 85 °C for 3 h. Samples were dried at 100 °C. Once cooled, 5 ml of 1% HNO_3 Ultrex (J.T. Baker) were added to completely dissolve the residue and then kept in a clean 10 ml tube. Ba and Mo isotopes were determined using a Thermo XSeries 2 ICP-MS with Indium as an internal standard. Standard additions were carried out on each tissue of an individual caught the first day of the experiment in order to check and correct the matrix effect. Certified reference material, dogfish liver DOLT-4 (NRCC) and lobster hepatopancreas TORT-2 (NRCC) were treated and analysed in the same way as the samples. The detection limits were 0.25 nmol g^{-1} dry weight for Mo and 0.10 nmol g^{-1} dry weight for Ba. For DOLT-4 and TORT-2, Mo values were in agreement with the expected values with a recovery of between 80 and 97% and a reproducibility of 2.3–11.7%. No data were available to certify the Ba quantification in the scallop soft tissue. Values obtained for Ba were 12.48 ± 0.57 nmol g^{-1} ($N = 12$) in TORT-2 and 0.706 ± 0.018 nmol g^{-1} ($N = 2$) in DOLT-4. Tissue metal concentrations are given on a dry weight basis (nmol g^{-1}).

2.5. Determination of Ba and Mo isotopes in shell by fs-LA-ICP-MS

Ba and Mo in scallop shells ($N = 70$) were analysed using an IR 1030 nm femtosecond laser (Alfamet-Novalase, France) in conjunction with an ELAN DRC II ICP-MS (Perkin Elmer). The ablation strategy chosen is a linear raster 2D scan as described in a previous study (Tabouret et al., 2010). This strategy produced a large ablation (400 μm in this study) while keeping a high spatial resolution (beam diameter: 17 μm) and limiting the mixing phenomenon between the calcareous increments being analysed. This method is applied from the experimental growth stop point to the edge of the shell along the growth axis and perpendicular to the daily growth increments. Differences in operating conditions from those described in Tabouret et al. (2010) are listed in Table 1. External calibrations for Ba and Mo were performed using certified glasses: NIST614, NIST612 and NIST610 (NIST, USA). Analytical accuracy was achieved with the fish otolith CRM NIES22 (NIES, Japan; Yoshinaga et al., 2000). Variation in ablation yield was checked using ^{43}Ca as an internal standard for each ablation; the instrumental drift was followed using ^{103}Rh in the nebulisation solution. Ba results from NIES analyses displayed recoveries from 92.5 to 112% and a reproducibility of around 10%. No certified or reference Mo values were available at this time. All concentrations were expressed as an Element/Ca ratio dividing shell elemental concentrations by the assumed calcium concentration in the shell (400 mg g^{-1}) and expressed in units of μmol $molCa^{-1}$ (Barats et al., 2007, 2009, 2010). Detection limits (nmol $molCa^{-1}$) calculated were: ^{95}Mo: 0.52, ^{97}Mo: 0.78, ^{98}Mo: 0.40, ^{135}Ba: 0.56, ^{137}Ba: 0.64 and ^{138}Ba: 1.96.

Table 1
Operating conditions of the fs-LA-ICP-MS.

Instrumentation	Femtosecond laser (Alfamet – Novalase, France)
Wavelength	1030 nm
Repetition rate	5000 Hz
Energy	45 μJ $pulse^{-1}$
Sampling strategy	Linear raster scan
Platine speed	5 μm s^{-1}
Scan speed	1000 μm s^{-1}
Gas flow (Helium)	100 ml min^{-1}
Isotopes and dwell times (ms)	^{95,97,98}Mo (200 ms), ^{103}Rh (20 ms), ^{135,137,138}Ba (50 ms), ^{43}Ca (20 ms)
Internal standard	^{43}Ca

The shells were photographed after ablation using an AxioCam MRc5 (Zeiss). A picture of the experimental sections was taken (×40) in order to date each part of the elemental profile. All the measurements showing the growth rates and the dates were performed using Visilog6 software (Noesis, France).

2.6. Data analysis

The bias linked to the isotopic impurities of the powders was taken into account and corrected for the water concentrations. The isotopic composition shift in soft tissue and shell was followed using enrichment isotope/natural isotope ratios.

2.6.1. Partition coefficient

The partition coefficients (D_{Ba} and D_{Mo}) were calculated before the first spike and for all the individuals as followed:

$$D_{Me} = [Me/Ca]_{shell} / [Me/Ca]_{water} \quad (2)$$

where D_{Me} is the partition coefficient for Mo or Ba, $[Me/Ca]_{shell}$ the Mo or Ba concentration in shell in μmol molCa^{-1}, and $[Me/Ca]_{water}$ the Mo or Ba total concentration in the water for the corresponding period in μmol molCa^{-1}.

2.6.2. Isotopic mass balance

The contribution of each isotopic spike to the total isotopic signature of water and the 6 biological compartments (gills, mantle, digestive gland, muscle, rest, shell) were estimated according to the following isotopic mass balance equation:

$$R_{mes} = a \cdot R_{nat} + b \cdot R_{spike} \quad (3)$$

for example: $R_{mes}(^{135}Ba/^{138}Ba) = a_{135Ba} * R_{nat}(^{135}Ba/^{138}Ba) + b_{135Ba} * R_{spike}(^{135}Ba/^{138}Ba)$where R_{mes} is the measured isotopic ratio in each compartment, to determine the contribution of each of the Ba and Mo spikes (e.g. $^{135}Ba/^{138}Ba$, $^{137}Ba/^{138}Ba$, $^{97}Mo/^{98}Mo$, $^{95}Mo/^{98}Mo$). "R_{nat}" is the natural isotopic ratio as measured before the addition of the various spikes. "R_{spike}" is the spike isotopic ratio as measured from the spiking solutions (e.g. $^{135}Ba/^{138}Ba$, $^{137}Ba/^{138}Ba$, $^{97}Mo/^{98}Mo$, $^{95}Mo/^{98}Mo$). "a" is the contribution (fraction) of endogenous ("natural") Ba or Mo in each compartment and "b" is the contribution (fraction) of the exogenous ("spiked") Ba or Mo.

Considering the relationship between both contributions as "$a + b = 1$", the spike contribution is:

$$b = \left[(R_{mes} - R_{nat})/R_{spike}\right] \Big/ \left[1 - \left(R_{nat}/R_{spike}\right)\right] * 100 \quad (4)$$

for example:

$$b_{135Ba} = \left[(R_{mes}(^{135}Ba/^{138}Ba) - R_{nat}(^{135}Ba/^{138}Ba)) / R_{spike}(^{135}Ba/^{138}Ba)\right] \Big/ \left[1 - \left(R_{nat}(^{135}Ba/^{138}Ba) / R_{spike}(^{135}Ba/^{138}Ba)\right)\right] * 100$$

The contributions were expressed in percentages. As each spike was also performed with different enriched isotopes for both Mo and Ba, overlapping between the calculated contributions based on isotopic ratio was possible, and independent mass balances could have been applied for each spiking condition.

2.6.3. Enrichment factor

The ability of the isotopes to incorporate into the soft tissue was also evaluated according to the enrichment factor (E.F.) with:

$$E.F. = [I^X]_{soft\ tissue} / [I^X]_{water} \quad (5)$$

where E.F. is the isotopic enrichment factor, $[I^X]_{soft\ tissue}$ the concentration of the isotope X in soft tissue and $[I^X]_{water}$ the concentration of the isotope X in the filtered water after the isotope X spike.

2.6.4. Growth rate effects

The effects of the growth rate on the incorporation of Ba and Mo were tested using a Pearson's regression analysis. We used ^{138}Ba concentration of the last shell increment versus the mean growth rate in the Mo tank (3 individuals per sampling) to test the effects on Ba incorporation, and ^{98}Mo concentration of the last shell increment versus mean growth rate (3 individuals per sampling) from the Ba tank to test the effects on Mo incorporation.

2.6.5. Statistical analyses

Finally, the relevance of the results obtained for water was checked with Kruskal Wallis non-parametrical tests. The significant differences among treatments of soft tissue were determined by analysis of variance (ANOVA) and compared using the Tukey HSD (Honestly Significant Difference) test. All statistical treatments were performed using the OriginPro8 software (OriginLab).

3. Results

3.1. Time-course evolution of the experimental conditions and scallop growth

The seawater temperature and salinity remained stable throughout the 16 days of the experiment in both tanks (Ba tank: 17.5 ± 0.8 °C; Mo tank: 17.4 ± 0.8 °C) (Ba tank: 34.9 ± 0.2; Mo tank: 34.6 ± 0.2). Oxygen saturation remained above 95% all the time.

The individual condition index decreased with time in both tanks. On Day 2, C.I. was 13.11 ± 0.59 ($N = 3$) and 12.54 ± 1.27 ($N = 3$) for individuals from the Mo and Ba tanks respectively. On Day 16, C.I. reached 7.78 ± 2.27 ($N = 3$) in the Mo tank and 9.00 ± 2.10 ($N = 3$) in the Ba tank.

The scallop shell length increased with a similar trend in both tanks between the field sampling and the end of the experiment (Fig. 1a) with a gain of 4.10 ± 0.24 mm and 3.90 ± 0.09 mm in the individuals sampled on the last day in the Ba and Mo tanks respectively. However, the growth rate was neither constant nor strictly similar in both tanks during the experiment (Fig. 1b). A maximum is observed on Day 13 in the Ba tank (0.42 ± 0.05 mm day^{-1}) and on Day 14 in the Mo tank (0.30 ± 0.15 mm day^{-1}). After these maxima, the rate of growth decreased to the end with a final growth rate of around 0.1 mm day^{-1}.

3.2. Evolution of the water isotopic composition

The evolution of the elemental composition of the dissolved phase matches with the evolution expected in the Ba and Mo tanks. In the Ba experiment, the total Ba concentrations in bulk samples were 10–12% higher than in the filtered samples illustrating a scavenging of the element (Fig. 2a, b). Despite such scavenging, the major part of the spikes remained in the dissolved phase and the shift of isotopic composition can be clearly distinguished after each isotopic enrichment. During the first two days of the experiment total Ba concentration in the dissolved phase was 37.5 ± 2.6 nmol l^{-1}. The concentration reached 178.6 ± 1.8 nmol l^{-1} after the ^{135}Ba enrichment and 432.2 ± 3.1 nmol l^{-1} after the ^{137}Ba spike (Fig. 2a, b).

In the Mo tank the comparison of the total Mo concentrations in the filtered and non-filtered samples indicate the absence of elemental scavenging by the particulate phase and/or on the tank surface over time-course of the experiment (Fig. 2c, d). Before the first enrichment, total Mo concentration reached 58.8 ± 1.2 nmol l^{-1}

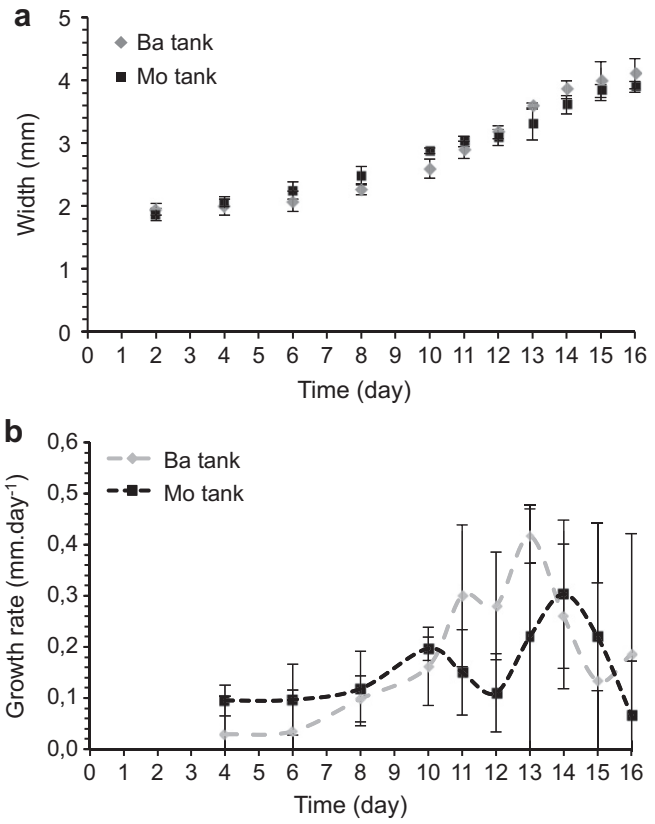

Fig. 1. Mean width gain (mm) (a) and growth rate (mm day^{-1}) (b) from the experimental growth stop until the sampling in Ba (grey diamond) and Mo (black square) tanks (3 individuals per analysis). Standard deviations are illustrated by double bars.

in the dissolved phase. The first ^{97}Mo spike induced an increase that reached 324.8 ± 4.8 nmol l^{-1} with a final concentration of 785.0 ± 12.6 nmol l^{-1} after the ^{95}Mo enrichment (Fig. 2c, d).

3.3. Assimilation of Mo and Ba in soft tissue

3.3.1. Elemental mass balance

Barium accumulation in mantle, gills and muscle increased as the dissolved Ba concentration in the tank water increased (Table 2):

$$[\mathrm{Ba}]_{\mathrm{mantle}} = 0.011[\mathrm{Ba}]_{\mathrm{water}} + 1.17 \qquad \left(r^2 = 0.9989\right) \qquad (6)$$

$$[\mathrm{Ba}]_{\mathrm{gills}} = 0.011[\mathrm{Ba}]_{\mathrm{water}} + 2.462 \qquad \left(r^2 = 0.8922\right) \qquad (7)$$

$$[\mathrm{Ba}]_{\mathrm{muscle}} = 9 \times 10^{-4}[\mathrm{Ba}]_{\mathrm{water}} + 0.346 \quad \left(r^2 = 0.9957\right) \qquad (8)$$

($[\mathrm{Ba}]_{\mathrm{tissue}}$ in nmol g^{-1} ww and $[\mathrm{Ba}]_{\mathrm{water}}$ in nmol l^{-1}). No significant relation was found for the digestive gland or the rest. The final concentrations were 3 times higher than the concentrations measured before the experiment for the gills and mantle and 2 times for the muscle. Approximately 50% of the total Ba load was found in the digestive gland, followed by the gills (~20%), the rest (~20%), the mantle (~15%) and the muscle (~3%) (Table 3). The proportion of Ba in the digestive gland, the rest and the muscle was unaffected by the dissolved Ba concentrations contrary to gills and mantle where the proportion of Ba increased with the dissolved Ba concentrations (Table 3).

The correlation between Mo concentrations in soft tissue and water was not significant in the Mo tank whatever the organ ($p > 0.005$; Table 2). Despite a slight increase in gills, mantle and muscle, the Mo concentrations in the soft tissue of individuals from the Mo and the Ba tank were very close. Most of the total Mo load (~85%) was found in the digestive gland, followed by the rest (~7%), the gills (~4%), the mantle (~2%), and the muscle (<1%).

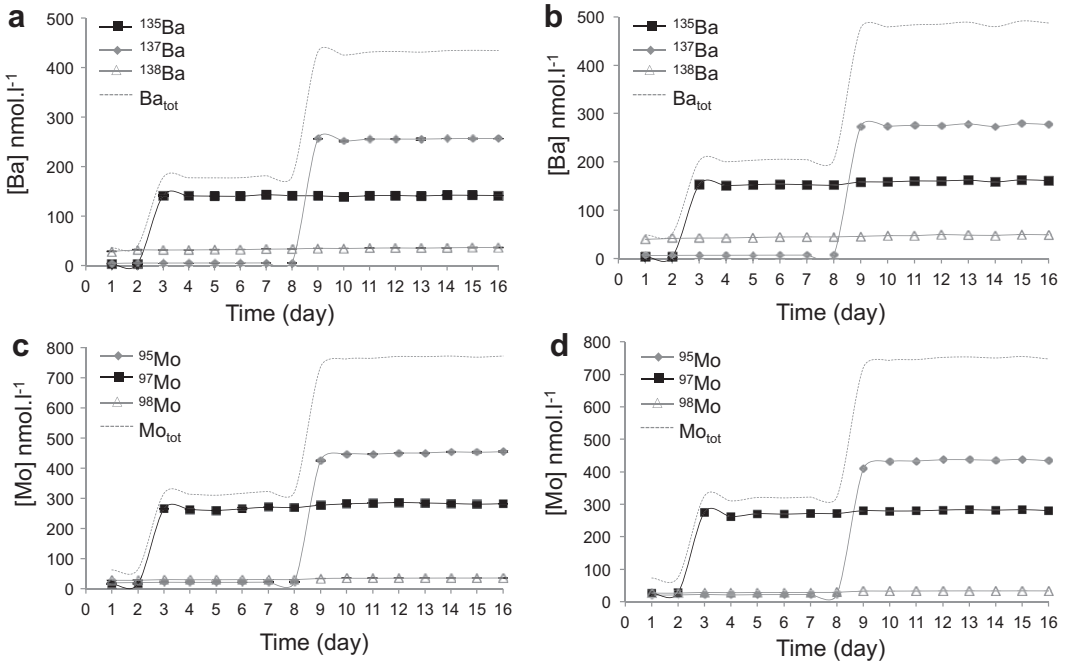

Fig. 2. Evolution of total Ba and Ba isotopes in filtered (a) and non-filtered water (b) in Ba tank, and of total Mo and Mo isotopes in filtered (c) and non-filtered water (d) in Mo tank. Standard deviations are illustrated by double bars.

Table 2
Mean Ba and Mo concentrations (nmol g^{-1} dry weight ± *standard deviation*) observed in *Pecten maximus* soft tissue exposed to dissolved Ba and Mo (nmol l^{-1}).

[*Me*] (nmol l^{-1})	Gills	Digestive gland	Mantle	Rests	Muscle
Ba					
Control 37.5 ± 2.6 ($N = 36$)	2.91 ± 0.92*a*	8.48 ± 1.56*a*	1.51 ± 0.44*a*	3.31 ± 1.34*a*	0.42 ± 0.09*a*
First spike 178.6 ± 1.8 ($N = 9$)	5.53 ± 0.56*b*	12.55 ± 0.73*b*	3.21 ± 0.01*b*	4.58 ± 1.30*b*	0.51 ± 0.05*a*
Second spike 432.2 ± 3.1($N = 21$)	7.46 ± 1.01*c*	10.74 ± 1.45*c*	6.65 ± 0.78*c*	4.47 ± 0.39*b*	0.82 ± 0.26*b*
Mo					
Control 58.8 ± 1.2 ($N = 36$)	14.21 ± 2.30*a*	298.87 ± 37.64	7.64 ± 0.89*a*	28.85 ± 2.70*a*	1.77 ± 0.64*a*
First spike 324.8 ± 4.8 ($N = 9$)	18.11 ± 3.64*b*	281.16 ± 56.51	8.37 ± 0.03*b*	33.0 ± 6.60*b*	2.56 ± 0.32*b*
Second spike 785.0 ± 12.6 ($N = 21$)	16.93 ± 1.93*b*	321.99 ± 70.85	9.03 ± 0.78*b*	24.72 ± 4.89*c*	2.84 ± 0.82*b*

Letters beside values indicate significant differences among treatments in each tank as determined by analysis of variance (ANOVA) ($p < 0.05$) and compared using the Tukey HSD test.

The proportion of Mo in each organ did not change significantly as the dissolved Mo concentrations in the exposure medium increased (Table 3).

3.3.2. Isotopic mass balance and enrichment factor

Before the enrichment, the Ba isotopic ratios were close to the natural ratios expected in both tanks ($Ba^{135}/Ba^{138} = 0.092$; $Ba^{137}/Ba^{138} = 0.157$). The shift of isotopic composition was observed in all the organs of the Ba tank individuals confirming the Ba assimilation (Fig. 3). For all the organs, the response occurred 2–3 days after the enrichment. The digestive gland response was lower than the other biological compartments (Fig. 3) with a contribution from both spikes of between 0.4 and 1.5% (Table 4). In gills, muscle and the rest, the contribution of the first spike was less than 1% and of the second spike 4 5% (Table 4). The maximum response to the Ba enrichments was observed in the mantle where the spike contribution was 2% for the first enrichment and 12.5% for the second (Table 4). However, the isotopic enrichment factor indicates no difference of incorporation ability between both isotopes (Table 4). The E.F. also highlights different incorporation abilities according soft tissue with digestive gland ≥ mantle ≥ gills > the rest > muscle.

Despite the absence of a relationship between soft tissue and total Mo concentrations in water, the isotopic compositions shifted during the experiment following the water enrichment (Fig. 3). Before the enrichments, the Mo isotopic ratios were close to the expected natural ratios. In the Mo tank, the isotopic signature of the digestive gland did not change significantly and remained close to the natural ratio values until the end, with a spike contribution below 0.1%. The response of the rest was also very low with a spike contribution below 0.1%. Gills, mantle and muscle reacted within 2 days of the isotopic enrichment. However, the isotopic contribution of both spikes was lower than the contribution observed in the Ba tank: less than 0.3% in gills and muscle, and 0.9% in mantle (Table 4). For a single soft tissue, no difference in isotopic enrichment factor was shown between the first and the second spikes (Table 4). The digestive gland showed the highest ability to incorporate Ba, followed by the rest, gills, mantle and muscle (Table 4).

3.4. Uptake of Ba and Mo isotopes by scallop shell as a function of time and isotopic composition of the water

3.4.1. Assimilation of Ba isotope

The regression analysis performed between the growth rate and ^{138}Ba revealed no influence of the growth rate on the Ba incorporation in shell ($R_{Pearson} = -0.3473$; $p = 0.2953$). The continuous Ba profiles revealed an increase in the total Ba concentration after both enrichments (Fig. 4a). Before the first spike, the total Ba concentration was 0.373 ± 0.079 μmol $molCa^{-1}$ ($N = 33$) and reached maximum values between 1.496 and 4.586 μmol $molCa^{-1}$ in the shells sampled after the second spike ($N = 21$). This increase is caused by the uptake of both Ba isotopes during the experiment. Fig. 4b illustrates the successive isotopic enrichments in shell due to the added fractions (^{135}Ba for the first spike, ^{137}Ba for the second spike) as a function of time. The ^{135}Ba concentration increased slightly after the first spike and increased dramatically 2 days after the second spike and finally levelled off (Fig. 4b). The ^{137}Ba concentration in the shell increased continuously after the second enrichment until the end of the experiment (Fig. 4b).

The Ba spike contribution in the shell indicated a similar pattern, with a levelling out of the ^{135}Ba after the second spike (Fig. 5). The ^{135}Ba spike contribution at this level state was around 5%. After the second spike, the ^{137}Ba contribution increased and reached 15% at the end of the experiment. Both contributions followed the general pattern of the ^{135}Ba and ^{137}Ba spike contributions in the water and in the mantle. The spike contributions in the shell were also in the same range as those observed in the mantle (^{135}Ba: 2.5%; ^{137}Ba: 14%) (Fig. 5).

The uptake of the dissolved Ba in the scallop shell can be divided into three parts based on the ^{135}Ba incorporation results and the observation of the daily increments of all the individuals from Ba tank. The ^{135}Ba incorporation, after the first enrichment, was observed in scallops sampled on Day 4 and indicated a turnover rate of less than one day. Before this date, and for the Mo tank individuals, the ^{135}Ba signal recorded by the carbonate matrix corresponds to the natural background signal and was 0.045 ± 0.018 μmol $molCa^{-1}$

Table 3
Relative Ba and Mo loads (% ± *standard deviation*) observed in *Pecten maximus* soft tissues exposed to dissolved Ba and Mo (nmol l^{-1}).

[*Me*] (nmol l^{-1})	Gills	Digestive gland	Mantle	Muscle	Rests
Ba					
Control 37.5 ± 2.6 ($N = 36$)	17 ± 5*a*	51 ± 8*a*	9 ± 2*a*	3 ± 1*ab*	20 ± 7*a*
First spike 178.6 ± 1.8 ($N = 9$)	21 ± 2*b*	48 ± 4*a*	12 ± 1*b*	2 ± 1*b*	17 ± 4*ab*
Second spike 432.2 ± 3.1 ($N = 21$)	25 ± 3*b*	36 ± 3*b*	22 ± 3*c*	3 ± 1*a*	15 ± 1*ab*
Mean ($N = 66$)	20 ± 5	46 ± 9	14 ± 6	3 ± 1	18 ± 6
Mo					
Control 58.8 ± 1.2 ($N = 36$)	3 ± 1*b*	89 ± 3*a*	2 ± 0.3*a*	0.5 ± 0.1*a*	6 ± 2*a*
First spike 324.8 ± 4.8 ($N = 9$)	5 ± 1*a*	82 ± 2*b*	2 ± 0.5*b*	0.7 ± 0.1*b*	10 ± 3*b*
Second spike 785.0 ± 12.6 ($N = 21$)	5 ± 1*a*	85 ± 2*c*	2 ± 0.5*b*	0.8 ± 0.2*b*	7 ± 2*a*
Mean ($N = 66$)	4 ± 1	87 ± 4	2 ± 0.5	0.6 ± 0.2	7 ± 2

Letters beside values indicate significant differences among treatments in each tank as determined by analysis of variance (ANOVA) ($p < 0.05$) and compared using the Tukey HSD test.

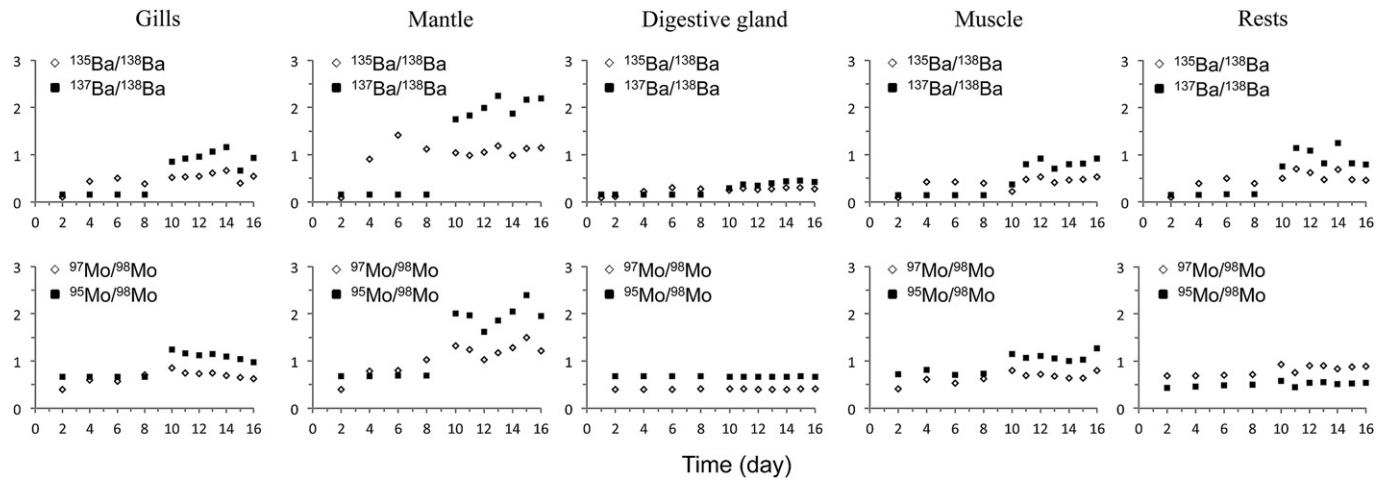

Fig. 3. Evolution of $^{97}Mo/^{98}Mo$, $^{95}Mo/^{98}Mo$ ratios in Mo tank and $^{135}Ba/^{138}Ba$, $^{137}Ba/^{138}Ba$ ratios in Ba tank in gills, mantle, digestive gland, muscle and the rest of *Pecten maximus* according time (day).

($N = 66$). During this phase the partition coefficient D_{135Ba} was 0.107 ± 0.026 ($N = 66$). The ^{135}Ba concentration increased continuously after the ^{135}Ba spike but increased dramatically after the ^{137}Ba spike. Considering the profiles of the scallops sampled on Days 14, 15 and 16 ($N = 9$), the increase took from 6 to 8 days to reach equilibrium. The mean concentration observed during the steady state was 0.939 ± 0.161 μmol molCa^{-1} ($N = 9$) and the D_{135Ba} was 0.068 ± 0.012.

For the second Ba isotope, the first ^{137}Ba signal increase appeared in the scallops sampled on Day 10 and indicated a time response of around 2 days. Due to experimental limitation of the scallop growth and development, the incubation was too short for the ^{137}Ba to reach a steady state.

3.4.2. Assimilation of Mo isotopes

According to the regression analysis, there was a significant trend of decreasing ^{98}Mo concentrations with increasing growth rate (f(growth rate) $= -0.2063 \times$ (growth rate) $- 4.1693$; $R_{Pearson} = -0.6843$; $p = 0.0291$). The continuous profile of the total Mo concentration did not reveal a significant increase with regard to time even in the shells sampled at the end of the experiment (Fig. 6a). The total Mo concentration remained at the background level for the whole the experiment ($Mo_{tot} = 0.051 \pm 0.013$ μmol molCa^{-1}; $N = 33$) with a low partition coefficient ($D_{Mo} = 0.0049 \pm 0.0013$).

The observation of the ^{97}Mo and ^{95}Mo spike contributions in the shells sampled on Days 14, 15 and 16 indicated a late and low increase in ^{97}Mo with a first spike contribution less than 2% and a second spike contribution less than 1% (Fig. 6b) meaning that part of the dissolved Mo was late in being assimilated. Contrary to the Ba enrichment, the ^{97}Mo contribution never reached a steady state after the spike.

4. Discussion

4.1. Experimental achievements and limitations

The main challenge of this work was to achieve, for the first time, a laboratory enrichment experiment with the Great Scallop *P. maximus*, and to define the enrichment of the dissolved phases with the lowest disturbance to growth. The experiment took place during the natural growth period of the scallop just after the end of winter growth. The feeding strategy chosen allowed the individual to grow without interfering with the enrichment as shown by the steady dissolved concentration in the water after each spike and the absence of change in the isotopic composition in the digestive gland. All the individuals grew during the experiment indicating the suitability of using *P. maximus* as biological model in laboratory experiments.

The water Ba concentrations before the enrichments were close to the concentrations described for the Bay of Brest (58 ± 12 nmol l^{-1}; Lorrain, 2002) and for ocean water (from 32 to 150 nmol l^{-1}; Bruland, 1983) indicating that the elemental conditions in the tanks were representative of the composition of natural seawater. Even if the final water concentration after the second enrichment was 4 times

Table 4
Contribution (% ± standard deviation) of the natural (a) and the added fraction (b) to the total isotopic signature, and isotopic enrichment factor (E.F.) in soft tissue (gills, mantle, digestive gland, muscle and the rest) from Ba tank (Ba isotopes) and Mo tank (Mo isotopes) individuals.

		Ba tank				Mo tank			
		$^{135}Ba/^{138}Ba$ ($N = 30$)		$^{137}Ba/^{138}Ba$ ($N = 21$)		$^{97}Mo/^{98}Mo$ ($N = 30$)		$^{95}Mo/^{98}Mo$ ($N = 21$)	
		Natural	Spike 1	Natural	Spike 2	Natural	Spike 1	Natural	Spike 2
Gills	Contribution (%)	99.1 ± 0.2	0.9 ± 0.2	94.6 ± 1.0	5.4 ± 1.0	99.7 ± 0.1	0.3 ± 0.1	99.6 ± 0.1	0.4 ± 0.1
	E.F.		*11.9 ± 1.3*		*12.0 ± 1.4*		*17.0 ± 2.3*		*16.3 ± 1.9*
Mantle	Contribution (%)	97.8 ± 0.3	2.2 ± 0.3	87.5 ± 1.3	12.5 ± 1.3	99.4 ± 0.2	0.6 ± 0.2	99.1 ± 0.2	0.9 ± 0.2
	E.F.		*12.8 ± 1.3*		*12.9 ± 1.7*		*10.4 ± 0.8*		*10.2 ± 0.7*
Digestive gland	Contribution (%)	99.6 ± 0.1	0.4 ± 0.1	98.5 ± 0.4	1.5 ± 0.4	99.9 ± 0.01	<0.1	99.9 ± 0.01	<0.1
	E.F.		*14.4 ± 2.6*		*10.9 ± 1.9*		*229.6 ± 49.5*		*249.8 ± 58.1*
Muscle	Contribution (%)	99.3 ± 0.2	0.7 ± 0.2	95.7 ± 1.3	4.3 ± 1.3	99.7 ± 0.1	0.3 ± 0.1	99.7 ± 0.1	0.3 ± 0.1
	E.F.		*1.1 ± 0.2*		*0.5 ± 0.1*		*2.6 ± 0.7*		*2.7 ± 0.9*
Rest	Contribution (%)	99.1 ± 0.2	0.9 ± 0.2	94.6 ± 1.5	5.4 ± 1.5	99.9 ± 0.1	<0.1	99.9 ± 0.1	<0.1
	E.F.		*8.0 ± 1.4*		*7.2 ± 0.8*		*22.2 ± 5.5*		*20.7 ± 3.9*

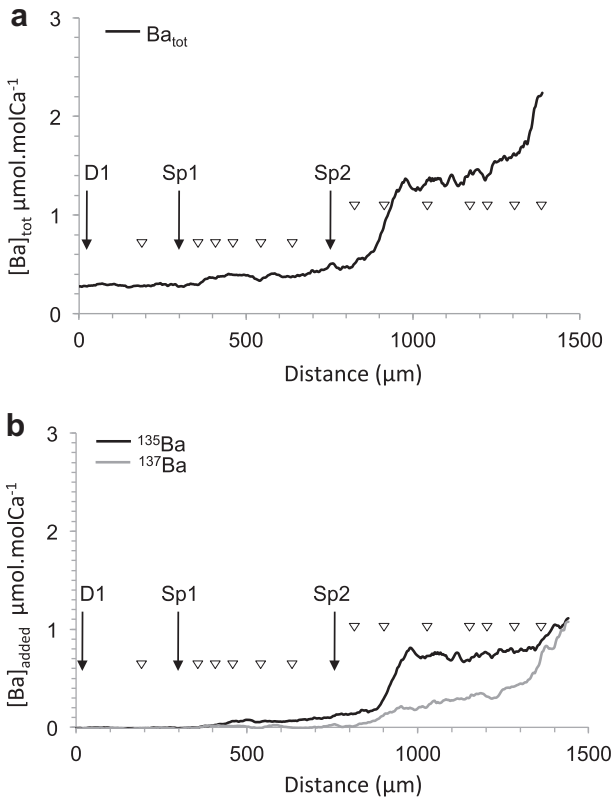

Fig. 4. Evolution of (a) total Ba concentration (µmol molCa^{-1}), and (b) added ^{135}Ba and ^{137}Ba concentration (µmol molCa^{-1}) in shell. D1: first day of the experiment; Sp1: day of ^{135}Ba spike (day 3); Sp2: day of ^{137}Ba spike (day 9). Other daily increments than D1, D3 and D9 are indicated by triangles.

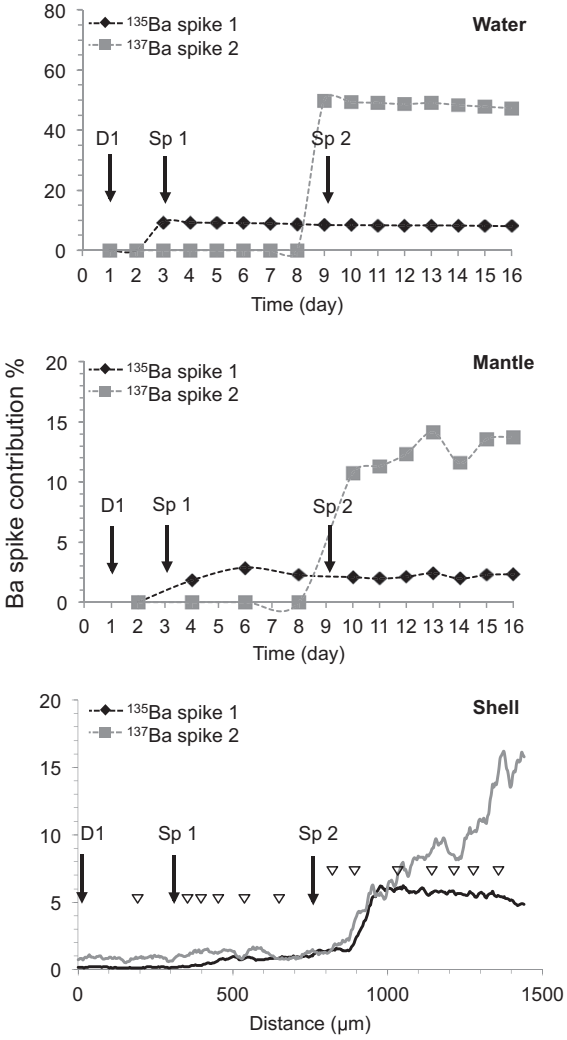

Fig. 5. Evolution of the ^{135}Ba from spike 1 and ^{137}Ba from spike 2 contribution (%) to the isotopic ratio in water, mantle and shell. D1: first day of the experiment; Sp1: day of ^{135}Ba spike (day 3); Sp2: day of ^{137}Ba spike (day 9). Other daily increments than D1, D3 and D9 in shell are indicated by triangles.

higher than the maximum values observed in the Bay of Brest in May and June 2000 (Lorrain, 2002), the concentration reached after the first spike was set to be closed to the maximum values observed in the Bay of Brest in May, June and August 2000 (Lorrain, 2002; Barats et al., 2009).

Mo water concentrations in both tanks were representative of the background concentrations of dissolved Mo. Recently measured concentrations ranged from 55 to 115 nmol l^{-1} in the water column in the Bay of Brest (Dulaquais, 2011). After the first spike, total Mo concentration was close to the concentration observed on the 12th May 2000 (428 ± 31 nmol l^{-1}) by Barats et al. (2010). The levels also fit with the concentration ranges recorded in the interstitial water in the Bay of Brest (from 70 to 500 nmol l^{-1}; Dulaquais, 2011). The time limitation induced by the experimental setup with a short incubation period (16 days) was probably too short to observe the whole kinetic incorporation of the ^{137}Ba and maybe both Mo isotopes. On the last day of the experiment individuals showed evidence of stress (low valve mobility, gill atrophy) illustrated by a decrease of both growth rate and condition index, probably due to a bacterial development linked to the absence of water renewal. This indicates that the experiment could not be extended.

4.2. Influence of the dissolved Ba in shell enrichment

4.2.1. Soft tissue assimilation and time response

The distribution of the Ba in the scallop soft tissue revealed the greatest concentration of Ba in the digestive gland supported by the highest enrichment factor. This is similar to the distribution observed in the species in the Bay of Brest (Barats, 2006) despite lower concentrations in the laboratory experiment (8.48 ± 1.56 nmol g^{-1} vs ~45 nmol g^{-1}). The difference observed for the concentrations may be due to the influence of Ba in the particulate phase in the field. Westerlund and Bechmann (2006) showed a dose dependant increase of Ba in gills and digestive gland of mussels and scallops exposed to three concentrations of drilling mud containing Ba. The "particulate phase" hypothesis is also consistent with the absence of correlation between dissolved Ba and digestive gland Ba concentrations. On the contrary, gills and mantle were sensitive to the dissolved Ba concentrations. In molluscs, biomineralization occurs within the extrapalleal fluid (EPF). The EPF is contained between the shell surface and the mantle epithelium (Wheeler, 1992). This medium is isolated and therefore may have different elemental concentrations to seawater. Elements move into the EPF through the epithelial mantle cells which are supplied from the hemolymph (Wilbur and Saleuddin, 1983). Gills are the first barrier allowing the passage of ions into the hemolymph. Several models have tried to explain the shell biomineralization by passive intercellular diffusion of ions into the EPF, i) active intracellular Ca-ATPase mediated pathway (Klein et al., 1996a,b), ii) Ca channels that preferentially select for Ca (Carré et al., 2006). In the latest model, as loading is increased these channels may transport Sr and Ba as well. High dissolved Ba concentrations may thus favour the transfer of the

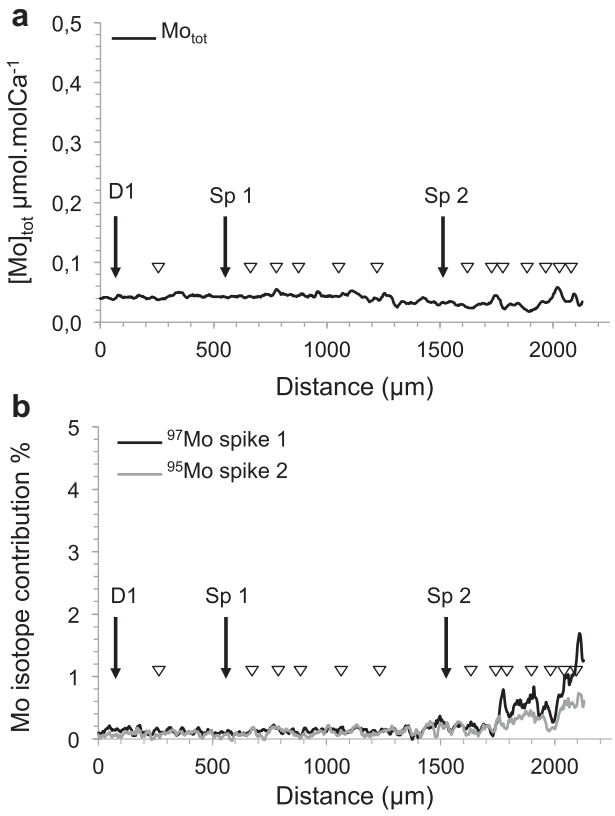

Fig. 6. Evolution of (a) total Mo concentration (µmol molCa^{-1}), (b) ^{97}Mo from spike 1 and ^{95}Mo from spike 2 contribution (%) to the isotopic ratio in shell. D1: first day of the experiment; Sp1: day of ^{135}Ba spike (day 3); Sp2: day of ^{137}Ba spike (day 9). Other daily increments than D1, D3 and D9 in shell are indicated by triangles.

element through the Ca channels in the mantle and an accumulation of Ba in the EPF initiating the shell enrichment. The concentration equilibrium in the mantle was reached in less than 3 days. However, this time was estimated to be 6–8 days for the shell.

This difference in the time response could be due to an analytical bias linked to the washout time for the ablation cell. Gas flow (helium) was optimised in order to limit the washout time. This is considered to be the time needed to recover the blank signal after the end of the ablation. The washout time was 10 s which corresponded approximately to a width of 50 µm based on the continuous scan sampling speed of 5 µm s^{-1}. However, the minimal daily growth rate of the scallops was 100 µm day^{-1}. This means that the error based on the washout time is less than half a day of the scallop life and does not explain the entire equilibration time. The difference in the time response may be associated with the time required for the EPF to reach equilibrium. The acceleration of the ^{135}Ba incorporation observed in the shell after the second spike may be due to the increase in Ba ions at the mantle epithelium surface induced by the second Ba enrichment. The accumulation of Ba ions at the mantle epithelium surface may reduce the competition between Ca, Sr and Ba ions for the Ca channels and favour the Ba, especially ^{135}Ba transfer from the medium to the EPF through the mantle. This suggests that Ba incorporation into the shell and the time response are highly dependent of the Ba availability in the surrounding environment. Further investigations are required to better understand this process. This time response can be considered to precisely date the elemental events recorded in the shell and to compare these signals with changes in the environmental conditions. For example, Barats et al. (2009) observed that Ba:Ca peaks in *P. maximus* tend to occur about a week after a Chl *a* peak. Considering the experimental time response of the bivalve shell, the two events probably occurred simultaneously.

4.2.2. Shell enrichment

In this study, no significant variation of Ba concentration was observed in the shell from Mo tank individuals despite the variability in growth rate. The regression analysis supports the absence of a growth rate influence on the Ba incorporation. Carré et al. (2006) indicated that in *M. donacium* and *C. subrugosa*, the crystal growth rates have an influence on the Sr incorporation in the shell. Nevertheless, their study showed that Ba incorporation is expected to be more dependent on its availability than on the growth rate. In *P. maximus* from the Bay of Brest, Barats et al. (2009) showed that Ba/Ca maxima in the shell were not due to shell growth anomaly and that Ba/Ca maxima cannot be directly related to minima of shell growth rate. Background concentrations recorded by the shell before the enrichments were similar to those found in *P. maximus* in the Bay of Brest, in other sites (Gillikin et al., 2008; Barats et al., 2009; Richard, 2009) but also in other pectinids like *C. radula* and *A. purpuratus* from tropical areas (Thébault, 2005) with concentrations ranging from 0.44 to 0.68 µmol molCa^{-1}. Background Ba:Ca ratio in mussel *M. edulis* shells were previously shown to be directly related to the Ba:Ca ratios in the water in which they grew (Gillikin et al., 2006). In our experiment the Ba partition coefficients were the same as those estimated by Barats et al. (2009) for *P. maximus* ($D_{Ba} = 0.11 \pm 0.03$) in the Bay of Brest. These values were also similar to D_{Ba} determined for *M. edulis* in laboratory (0.10 ± 0.02) and field experiments (0.071 ± 0.001) (Gillikin et al., 2006) and confirmed by an experimental approach showing that Ba background in *P. maximus* shells may be considered as a relevant proxy of Ba aqueous concentration.

The major pool of Ba in seawater at the sediment water interface (SWI) originates from the dissolved phase. Variations of dissolved and particulate phases of Ba exhibit concentration ranges from 45 to 100 nmol l^{-1} and from 0.7 to 9 nmol l^{-1} respectively in the Bay of Brest (Barats et al., 2009). It was therefore important to verify to what extent the dissolved phase was involved in the calcite Ba maximum. The 12 fold increase in the Ba concentration in water induced a 4–12 fold increase of the total Ba concentration in the shell. The maxima observed at the end of the experiment (from 1.5 to 4.6 µmol molCa^{-1}) were similar to the maxima observed in *P. maximus* from other ecosystems (Bay of Brest, Belle Ile, Bay of Seine, Ria de Vigo) ranging from 0.73 to 5.5 µmol molCa^{-1} (Barats et al., 2009; Gillikin et al., 2008) but also in other species caught in temperate and tropical ecosystems (Barats et al., 2009). The total Ba concentration in the shell never reached equilibrium despite an early stabilization of the total Ba concentration in water. This is due to the non equilibrium state of the ^{137}Ba concentration at the end of the experiment. However, the ^{135}Ba concentration reached equilibrium with the water concentration 6–8 days after the enrichment and allowed the estimation of the final D_{135Ba}. The values provided (0.068 ± 0.012) were close to the background D_{Ba} values of this study and within the range described in the literature (Barats et al., 2009; Gillikin et al., 2006). The difference observed between the D_{Ba} before the spike and after the spike is in the same range as the difference observed between laboratory grown and field grown *M. edulis* by Gillikin et al. (2006). As an explanation, Gillikin et al. suggested that the sudden increase in Ba concentration in the laboratory experiment caused a saturation of the ionoregulation ability of the animal. For the same bivalve species, Lorens and Bender (1980) found that elemental ratios in shells increased in laboratory held individuals for a short while, then decreased. They proposed that this was caused by the stress of capture and the adjustment to a new environment. We also suggest that the laboratory experimental conditions with no water renewal and specific food given at a specific frequency may change the metabolic rate. Nevertheless,

the D_{Ba} value after the spike is very close to the inorganic D_{Ba} given by Pingitore and Eastman (1984) (0.06 ± 0.01) and supports the use of Ba as an environmental proxy. These results demonstrate that a significant increase in the dissolved Ba concentrations can essentially explain the Ba maxima observed in the Great Scallop shell.

Ba:Ca peaks in bivalve shells are often considered to be linked to primary productivity (Stecher et al., 1996; Vander Putten et al., 2000; Lazareth et al., 2003). Stecher and Kogut (1999) propose that a release of barium happens quickly after at the end of a bloom in an estuary, following the phytoplankton decay and sedimentation. Most of the barium released after a bloom is labile and only a minor fraction forms barite crystals (Ganeshram et al., 2003). Our experimental results, agree with these observations suggesting an incorporation of Ba from phytoplankton bloom through the dissolved phase.

However, in most of the studies dealing with pectinids' microchemistry, the maxima do not always coincide with phytoplankton bloom (Gillikin et al., 2008; Barats et al., 2009). The turnover rate linked to the environmental conditions could be at the origin of the non synchronicity when phytoplankton bloom and Ba maxima in the shell are separated by only one or two weeks. Finally, the occurrence of Ba maxima in shell without significant phytoplankton bloom may suggest other enrichment processes of the dissolved phase in the environment surrounding the shell (e.g. sediment–water interface).

4.3. Influence of the aqueous phase in Mo uptake

4.3.1. Soft tissue assimilation and time response

In the individuals sampled from the Mo tank, the digestive gland displayed the highest Mo concentration and enrichment factor. The levels observed in this organ were higher than those observed in *Chlamys varia* from the Bay of Biscay (~ 60 nmol g^{-1}; Bustamante and Miramand, 2005). As for *C. varia*, the digestive gland accounts for the majority of the Mo body load, up to 89%. Our results were also similar to those obtained with *P. maximus* from the bay of Brest (Brittany, French Coast) with concentrations around 160 nmol g^{-1} and the digestive gland represents 69% of the total Mo in the bivalve (soft tissue and shell) (Barats et al., 2010). Nørum et al. (2005) found that the Mo content in the digestive gland of the Spiny and Pacific Scallops was one order of magnitude higher than in gills. Most of the Mo found in the digestive gland seems to be situated in the cytosolic fraction (Bustamante and Miramand, 2005). The organ was not sensitive to the dissolved Mo increase and was not affected by the shift of the water isotopic composition indicating the role of the digestive gland is only in dietary Mo uptake. The concentrations and contributions of the other organs analysed were very close to those described in *C. varia* from the Bay of Biscay (Bustamante and Miramand, 2005) and *P. maximus* from the Bay of Brest (Barats, 2006) with very low contribution to the Mo load compared to the digestive gland. Even if these organs did not display a relationship to the dissolved Mo concentrations, they were affected by the shift in the isotopic composition. No accumulation was observed; the variation in isotopic composition may be due to a preferential incorporation or adsorption, of the major isotope available in the surrounding medium, at the tissue surface.

4.3.2. Shell enrichment

The regression analysis between growth rate versus Mo concentrations in shell suggests an influence of the growth rate on the Mo incorporation. However, Barats et al. (2010) indicated that the growth rate cannot explain the intense spring peak of Mo observed in *P. maximus* from the Bay of Brest. This relationship has thus to be confirmed with further investigations.

Background concentrations recorded by the shell before the enrichments were higher than concentrations indirectly estimated by Barats et al. (2010) in *P. maximus* from the Bay of Brest but in the same range as concentrations found by Thébault et al. (2009) in *C. radula* from New Caledonia. The more accurate value obtained in our laboratory experiment (D_{Mo} = 0.0049 ± 0.0013) than in the field confirms the low partition coefficient D_{Mo} expected for *P. maximus*. The main difference with the value estimated by Barats et al. ($D_{Mo} = 1.5 \times 10^{-4}$) is due to Mo:Ca values in the shells being systematically below the detection limit. Nevertheless, such low D_{Mo} values are consistent with a strong limitation of Mo precipitation pathway in an anionic form within the calcareous matrix (Barats et al., 2010).

High increases of Mo were recently observed at the SWI in the Bay of Brest (Dulaquais, 2011) and the concentrations match the levels used in the present study (70–500 nmol L^{-1}). Despite a slight shift in the Mo isotopic composition at the end of the experiment, the shells were not sensitive to the dissolved Mo increase and stayed at the background level. These results in association with the soft tissue observations, provide the evidence that the spring enrichments found in shells of wild populations cannot be explained by direct dissolved Mo uptake and are likely to have a dietary origin. Scallop ingestion of suspended particles would result in a Mo ion accumulation, first in the hemolymph, then in the EPF and finally in the calcite shell. The relative contribution of Mo to the shell, from food sources versus the environment is unknown and further experiments on Mo dietary uptake would be useful. A separate isotopic labelling of each compartment (water, food) would help in the distinction of their respective contribution to shell enrichment.

5. Conclusion

The influence of the dissolved Ba and Mo concentrations on the bivalve shell enrichment was investigated in an original laboratory experiment using young scallop shells and isotopic tracers. Despite its sensitive growth, the Great Scallop was found to be a suitable biological model that grew throughout the experiment and produced daily increments delivering a high resolution record. This ability gives a biological model and a wide range of tests to give a better understanding of the record of elemental signals in the shells. Isotopic tracers helped to understand the Ba and Mo uptake in soft tissue and shells. Moreover the use of two successive isotope enrichments for each element is an original way to evaluate the incorporation kinetics. Results confirmed that the major role of the dissolved phase is in the Ba incorporation in the shell. Results also revealed that the time response of the shell to record the water enrichment was about one week (±1 day). The low D_{Mo} (0.046 ± 0.013), the absence of Mo increase and spike contribution to the total isotopic signal in shells after the water enrichment, clearly indicate that the dissolved Mo cannot be at the origin of the Mo peaks in the Bay of Brest. Finally, further studies on the specific role of the particulate phase to promote the Mo seasonal peaks in bivalve shell, and on the accumulation of dissolved Ba at the SWI, are required to better understand the biogeochemistry of these elements and their potential use as environmental proxies.

Acknowledgements

The authors are grateful to the staff from the Tinduff hatchery for their help with experimental design and scallop feeding. Thanks to Antoine Carlier for his help with experimental logistics. We would like to thank Matthieu Waeles from LEMAR (Brest), Emmanuel Tessier and Gilles Bareille from LCABIE (Pau) for their help in the elemental analyses. This work and H. Tabouret's postdoctoral fellowship were supported in the framework of the CHIVAS project

funded by the French National Research Agency (ANR "Blanc" programme).

References

Averyt, K.B., Paytan, A., 2004. A comparison of multiple proxies for export production in the equatorial Pacific. Paleoceanography 19 (PA4003). doi:10.1029/2004PA001005.

Barats, A., 2006. Microanalyse quantitative des éléments traces dans la calcite de la coquille St Jacques (*Pecten maximus*) par Ablation Laser ICP-MS: une archive journalière de la biogéochimie des environnements côtiers tempérés. Université de Pau et des Pays de l'Adour, Pau. 326p.

Barats, A., Amouroux, D., Chauvaud, L., Pécheyran, C., Lorrain, A., Thébault, J., Church, T., Donard, O.F.X., 2009. High frequency Barium profiles in shells of the Great Scallop *Pecten maximus*: a methodical long-term and multi-site survey in Western Europe. Biogeosciences 6, 157–170.

Barats, A., Amouroux, D., Pécheyran, C., Chauvaud, L., Donard, O.F.X., 2008. High frequency archives of Manganese inputs to coastal waters (Bay of Seine, France) resolved by the LA-ICP-MS analysis of calcitic growth layers along Scallop shells (*Pecten maximus*). Environmental Science and Technology 42, 86–92.

Barats, A., Amouroux, D., Pécheyran, C., Chauvaud, L., Thébault, J., Donard, O.F.X., 2010. Spring molybdenum enrichment in scallop shells: a potential tracer of diatom productivity in temperate coastal environments (Brittany, NW France). Biogeosciences 7, 233–245.

Barats, A., Pécheyran, C., Amouroux, D., Dubascoux, S., Chauvaud, L., Donard, O.F.X., 2007. Matrix-matched quantitative analysis of trace-elements in calcium carbonate shells by laser-ablation ICP-MS: application to the determination of daily scale profiles in scallop shell (*Pecten maximus*). Analytical and Bioanalytical Chemistry 387, 1131–1140.

Bruland, K.W., 1983. Trace elements in seawater. In: Riley, J.P., Chester, R. (Eds.), 1983. Chemical Oceanography, vol. 8. Academic Press, pp. 157–220.

Bustamante, P., Miramand, P., 2005. Subcellular and body distributions of 17 trace elements in the variegated scallop *Chlamys varia* from the French coast of the Bay of Biscay. Science of the Total Environment 337, 59–73.

Carré, M., Bentaleb, I., Bruguier, O., Ordinola, E., Barrett, N.T., Fontugne, M., 2006. Calcification rate influence on trace element concentrations in aragonite bivalve shells: evidences and mechanisms. Geochimica et Cosmochimica Acta 70, 4906–4920.

Chauvaud, L., Lorrain, A., Dunbar, R.B., Paulet, Y.M., Thouzeau, G., Jean, F., Guarini, J.M., Mucciarone, D., 2005. The shell of the great scallop *Pecten maximus* as a high frequency archive of paleoenvironmental change. Geochemistry Geophysics Geosystems 6, Q08001.

Chauvaud, L., Thouzeau, G., Paulet, Y.M., 1998. Effects of environmental factors on the daily growth rate of *Pecten maximus* juveniles in the Bay of Brest (France). Journal of Experimental Marine Biology and Ecology 227, 83–111.

Dodd, J.R., 1965. Environmental control of strontium and magnesium in *Mytilus*. Geochimica Cosmochimica Acta 29, 385–398.

Dulaquais, G., 2011. Etude comportementale du molybdène en milieu estuarien: Estuaire de l'Aulne – Rade de Brest. In: Rapport de stage M2, Master SCEM. Université de Bretagne Occidentale – IUEM. 26p.

Epplé, V.M., 2004. High-Resolution Climate Reconstruction for the Holocene Based on Growth Chronologies of the Bivalve *Artica islandica* from the North Sea. Department of Geosciences, University of Bremen, Bremen, Germany. 101p.

Freitas, P., Clarke, L.J., Kennedy, H., Richardson, C., Abrantes, F., 2006. Environmental and biological controls on elemental (Mg/Ca, Sr/Ca and Mn/Ca) ratios in shells of the king scallop *Pecten maximus*. Geochimica Cosmochimica Acta 70, 5119–5133.

Fritz, L.W., Ragone, L.M., Lutz, R.A., 1990. Biomineralization of barite in the shell of the freshwater Asiatic clam *Corbicula fluminea* (Mollusca: Bivalvia). Limnology and Oceanography 35, 756–762.

Ganeshram, R.S., Francois, R., Commeau, J., Brown-Leger, S.L., 2003. An experimental investigation of barite formation in seawater. Geochimica Cosmochimica Acta 70, 4617–4634.

Gillikin, D.P., Dehairs, F., Lorrain, A., Steenmans, D., Baeyens, W., Andre, L., 2006. Barium uptake into the shells of the common mussel (*Mytilus edulis*) and the potential for estuarine paleo-chemistry reconstruction. Geochimica Cosmochimica Acta 70, 395–407.

Gillikin, D.P., Lorrain, A., Navez, J., Taylor, J.W., André, L., Keppens, E., Baeyens, W., Dehairs, F., 2005. Strong biological controls on Sr/Ca ratios in aragonitic marine bivalve shells. Geochemistry Geophysics Geosystems 6, Q05009. doi:10.1029/2004GC000874.

Gillikin, D.P., Lorrain, A., Paulet, Y.M., André, L., Dehairs, F., 2008. Synchronous barium peaks in high-resolution profiles of calcite and aragonite marine bivalve shells. Geo-Marine Letters 28, 351–358.

Klein, R.T., Lohmann, K.C., Thayer, C.W., 1996a. Bivalve skeletons record sea-surface temperature and delta O-18 via Mg/Ca and O-18/O-16 ratios. Geology 24, 415–418.

Klein, R.T., Lohmann, K.C., Thayer, C.W., 1996b. Sr/Ca and 13C/12C ratios in skeletal calcite of *Mytilus trossulus*: covariation with metabolic rate, salinity, and carbon isotopic composition of seawater. Geochimica Cosmochimica Acta 60, 4207–4221.

Lazareth, C.E., Vander Putten, E., André, L., Dehairs, F., 2003. High resolution trace element profiles in shells of the mangrove bivalve *Isognomon ephippium*: a record of environmental spatio-temporal variations? Estuarine Coastal Shelf Sciences 57, 1103–1114.

Lorens, R.B., Bender, M.L., 1980. The impact of solution chemistry on *Mytilus edulis* calcite and aragonite. Geochimica Cosmochimica Acta 44, 1265–1278.

Lorrain, A., Gillikin, D.P., Paulet, Y.M., Chauvaud, L., Le Mercier, A., Navez, J., André, L., 2005. Strong kinetic effects on Sr/Ca ratios in the calcitic bivalve *Pecten maximus*. Geology 33, 965–968.

Lorrain, A., 2002. Utilisation de la coquille Saint-Jacques comme un traceur environnemental: approches biologique et biogéochimique. Institut Universitaire Européen de la Mer, Université de Bretagne Occidentale, Plouzané, 289 pp.

McCulloch, M., Fallon, M., Wyndham, T., Hendy, E., Lough, J., Barnes, D., 2003. Coral record of increased sediment flux to the inner Great Barrier Reef since European settlement. Nature 421, 727–730.

Nørum, U., Lai, V.W.M., Cullen, W.R., 2005. Trace element distribution during the reproductive cycle of female and male spiny and Pacific scallops, with implications for biomonitoring. Marine Pollution Bulletin 50 (2), 175–184.

Pingitore, N.E., Eastman, M.P., 1984. The experimental partitioning of Ba^{2+} into calcite. Chemical Geology 45, 113–120.

Richard, M., 2009. Analyse de la composition élémentaire de *Pecten maximus* par HR-ICP-MS Element 2: développements méthodologiques et interprétations écologiques. Institut Universitaire Européen de la Mer, Université de Bretagne Occidentale, Plouzané. 264p.

Schöne, B.R., Pfeiffer, T., Pohlmann, T., Siegismund, F., 2005. A seasonally resolved bottom-water temperature record for the period AD 1866-2002 based on shells of *Artica islandica* (Mollusca, North Sea). International Journal of Climatology 25, 947–962.

Sinclair, D.J., McCulloch, M.T., 2004. Corals record low mobile barium concentrations in the Burdekin River during the 1974 flood: evidence for limited Ba supply to rivers? Paleogeography, Paleoclimatology, Paleoecology 214, 155–174.

Smith, S.V., Hollibaugh, J.T., 1993. Coastal metabolism and the oceanic organic carbon balance. Review of Geophysics 31, 75–89.

Stecher, H.A., Kogut, M.B., 1999. Rapid barium removal in the Delaware estuary. Geochimica Cosmochimica Acta 63, 1003–1012.

Stecher, H.A., Krantz, D.E., Lord, C.J., Luther, G.W., Bock, K.W., 1996. Profiles of strontium and barium in *Mercenaria mercenaria* and *Spisula solidissima* shells. Geochimica Cosmochimica Acta 60, 3445–3456.

Tabouret, H., Bareille, G., Claverie, F., Pécheyran, C., Prouzet, P., Donard, O.F.X., 2010. Simultaneous use of strontium:calcium and barium :calcium ratios in otoliths as markers of habitat: application to the European eel (*Anguilla anguilla*) in the Adour basin, South West France. Marine Environmental Research 70, 35–45.

Thébault, J., 2005. La coquille de *Comptopallium radula* (Bivalvia ; Pectinidae), archive eulérienne haute fréquence de la variabilité de l'environnement côtier tropical (Océan Pacifique). Institut Universitaire Européen de la Mer, Université de Bretagne Occidentale, Plouzané. 277p.

Thébault, J., Chauvaud, L., L'Helguen, S., Clavier, J., Barats, A., Jacquet, S., Pécheyran, C., Amouroux, C., 2009. Barium and molybdenum records in bivalve shells: geochemical proxies for phytoplankton dynamics in coastal environments? Limnology and Oceanography 54, 1002–1014.

Vander Putten, E., Dehairs, F., Keppens, E., Baeyens, W., 2000. High resolution distribution of trace elements in the calcite shell layer of modern *Mytilus edulis*: environmental and biological controls. Geochimica Cosmochimica Acta 64, 997–1011.

Westerlund, S., Bechmann, R.K., 2006. Metals in tissues of mussels, scallops and cod exposed to suspended particles of water based drilling mud. In: Bechmann, R.K. (coord.) (Ed.), Impacts of Drilling Mud Discharges on Water Column Organism and Filter Bivalves. Report IRIS 72p.

Wheeler, A., 1992. Mechanisms of molluscan shell formation. In: Bonucci, E. (Ed.), Calcification in Biological Systems. CRC, Boca Raton, pp. 179–216.

Wilbur, K.M., Saleuddin, A.S.M., 1983. Shell formation. In: Bonucci, E. (Ed.), The Mollusca. Academic Press, New York, pp. 235–287.

Yoshinaga, J., Nakama, A., Morita, M., Edmonds, J.S., 2000. Fish otolith reference material for quality assurance of chemical analyses. Marine Chemistry 69 (1–2), 91–97.